Published in final edited form as:
J Immunol. 2008 November 15; 181(10): 7390–7399.

Intestinal Macrophage/Epithelial Cell-Derived CCL11/Eotaxin-1 Mediates Eosinophil Recruitment and Function in Pediatric Ulcerative Colitis[1]

Richard Ahrens[*], **Amanda Waddell**[*], **Luqman Seidu**[*], **Carine Blanchard**[*], **Rebecca Carey**[†], **Elizabeth Forbes**[*], **Maria Lampinen**[‖], **Tara Wilson**[†], **Elizabeth Cohen**[*], **Keith Stringer**[‡], **Edgar Ballard**[‡], **Ariel Munitz**[*], **Huan Xu**[§], **Nancy Lee**[¶], **James J. Lee**[¶], **Marc E. Rothenberg**[*], **Lee Denson**[†], and **Simon P. Hogan**[*,2]

[*] Division of Allergy and Immunology, University of Cincinnati College of Medicine, CCHMC, Cincinnati, OH 45229

[†] Division of Gastroenterology, Hepatology and Nutrition, University of Cincinnati College of Medicine, CCHMC, Cincinnati, OH 45229

[‡] Division of Pathology, University of Cincinnati College of Medicine, CCHMC, Cincinnati, OH 45229

[§] Division of Biomedical Informatics, Department of Pediatrics, University of Cincinnati College of Medicine, CCHMC, Cincinnati, OH 45229

[¶] Division of Pulmonary Medicine, Mayo Clinic Arizona, Scottsdale, AZ 85259

[‖] Department of Medical Sciences, University of Uppsala, Uppsala, Sweden

Abstract

Clinical studies have demonstrated a link between the eosinophil-selective chemokines, eotaxins (eotaxin-1/CCL11 and eotaxin-2/CCL24), eosinophils, and the inflammatory bowel diseases, Crohn's disease and ulcerative colitis (UC). However, the cellular source and individual contribution of the eotaxins to colonic eosinophilic accumulation in inflammatory bowel diseases remain unclear. In this study we demonstrate, by gene array and quantitative PCR, elevated levels of eotaxin-1 mRNA in the rectosigmoid colon of pediatric UC patients. We show that elevated levels of eotaxin-1 mRNA positively correlated with rectosigmoid eosinophil numbers. Further, colonic eosinophils appeared to be degranulating, and the levels positively correlated with disease severity. Using the dextran sodium sulfate (DSS)-induced intestinal epithelial injury model, we show that DSS treatment of mice strongly induced colonic eotaxin-1 and eotaxin-2 expression and eosinophil levels. Analysis of eosinophil-deficient mice defined an effector role for eosinophils in disease pathology. DSS treatment of eotaxin-$2^{-/-}$ and eotaxin-$1/2^{-/-}$ mice demonstrated that eosinophil recruitment was dependent on eotaxin-1. In situ and immunofluorescence analysis-identified eotaxin-1 expression was restricted to intestinal $F4/80^{+}CD11b^{+}$ macrophages in DSS-induced epithelial injury and to $CD68^{+}$ intestinal macrophages and the basolateral compartment of intestinal epithelial cells in pediatric UC. These data demonstrate that intestinal macrophage and epithelial cell-derived eotaxin-1 plays a critical role

[1]This work was supported in part by Crohn's Colitis Foundation of American Career Development Award 2007 (to S.P.H.), Digestive Disease Health Center Pilot and Feasibility Research Grant of the National Institutes of Health-supported Cincinnati Children's Hospital Research Foundation Digestive Health Center (1P30DK078392-01) (to S.P.H.), and National Institutes of Health Grant R01 DK058259 (to L.D.).

2Address correspondence and reprint requests to Dr. Simon P. Hogan, Division of Allergy and Immunology, Cincinnati Children's Hospital Medical Center, 3333 Burnet Avenue, ML7028, Cincinnati OH 45229. E-mail address: simon.hogan@cchmc.org.

Disclosures

The authors have no financial conflict of interest.

in the regulation of eosinophil recruitment in colonic eosinophilic disease such as pediatric UC and provides a basis for targeting the eosinophil/eotaxin-1 axis in UC.

The inflammatory bowel diseases (IBD)[3] Crohn's disease (CD) and ulcerative colitis (UC) are chronic, relapsing, and remitting gastrointestinal (GI) diseases that affect >5 million people in North America and Europe. It is currently believed that chronic inflammation of the GI tract predisposes to the clinical manifestations of disease, leading to the long-term and sometimes irreversible impairment of GI structure and function (1). A feature of the inflammation in GI tissue biopsy specimens from patients with IBD, particularly UC, is elevated levels of eosinophils (2). Although eosinophils usually represent only a small percentage of the infiltrating leukocytes (2,3), their level has been proposed to be a negative prognostic indicator (3,4).

Eosinophils are multifunctional leukocytes involved in the initiation and propagation of inflammatory reactions and the modulation of innate and adaptive immunity and can serve as a major effector cell, inducing tissue damage and dysfunction (5). Eosinophils may induce GI dysfunction through the release of lipid mediators and eosinophilic granular proteins (major basic protein (MBP), eosinophil peroxidase (EPO) and eosinophil-associated ribonucleases, i.e., eosinophil cationic protein (ECP) and eosinophil-derived neurotoxin (EDN)). The level of the eosinophil constituents MBP, EPO, ECP, and EDN have been shown to be elevated in adult IBD patients, and the level of these proteins correlated with disease severity (6,7). Eosinophil levels and involvement in the pathogenesis of pediatric UC has not yet been determined.

The trafficking of eosinophils into inflammatory sites has been shown to involve a number of cytokines (most notably the Th2 cell products (IL-4, IL-5, and IL-13) (8–10), adhesion molecules (e.g., β_1, β_2, and β_7 integrins) (11), chemokines (e.g., RANTES and the eotaxins) (12), and other recently identified molecules (e.g., acidic mammalian chitinase) (13). Of the cytokines implicated in modulating leukocyte recruitment, only IL-5 and the eotaxins selectively regulate eosinophil trafficking (14). IL-5 regulates growth, differentiation, activation, and survival of eosinophils (15); however, Ag-induced tissue eosinophilia can occur independently of IL-5 as demonstrated by residual tissue eosinophils in trials using anti-IL-5 in patients with asthma (16) and IL-5-deficient mice (17,18). Experimental investigations demonstrate that members of the eotaxin subfamily of CC chemokines, CCL11 (eotaxin-1), CCL24 (eotaxin-2), and CCL26 (eotaxin-3), selectively regulate eosinophil trafficking under both inflammatory and homeostatic conditions (5). Indeed, transgenic overexpression of eotaxin-1 in the GI tract promotes an intestinal eosinophilia (19). Furthermore, allergen-induced pulmonary eosinophilia and nematode-induced intestinal eosinophilia was dependent on eotaxin-1/eotaxin receptor CCR3 pathways (5,20). Using eotaxin-1 and eotaxin-2 single and double gene-deficient mice or neutralizing Abs, both chemokines have been shown to have nonoverlapping roles in regulating the temporal and regional distribution of eosinophils in pulmonary eosinophilic inflammation (21–23).

Clinical investigations have provided circumstantial data to suggest eotaxin-1 and eotaxin-2 involvement in IBD. Eotaxin-1 protein in serum of adult IBD patients has been shown to be elevated as compared with normal individuals (24,25). Furthermore, eotaxin-1 protein has been preliminarily identified in full thickness bowel wall biopsy samples of adult IBD patients (26). In addition, single nucleotide polymorphism analysis in a Korean population with UC revealed a significant difference in genotype and allele frequency of the eotaxin-2, but not

[3]Abbreviations used in this paper: IBD, Inflammatory bowel disease; CD, Crohn's disease; DSS, dextran sodium sulphate; EPO, eosinophil peroxidase; GI, gastrointestinal; hpf, high-powered field; UC, ulcerative colitis; UCHIS, UC histologic index of severity; WT, wild type.

eotaxin-3, gene in UC, suggesting an association between eotaxin-2 and susceptibility to UC (27). Eotaxin subfamily expression and the individual role of eotaxins in eosinophil recruitment in pediatric UC remains unclear.

In the present study we define the expression of eotaxin-1, eotaxin-2, and eotaxin-3 in pediatric UC. We show that eotaxin-1, and not eotaxin-2 or eotaxin-3, is elevated in rectosigmoid biopsy samples from pediatric UC patients. Further, we show that elevated levels of eotaxin-1 positively correlated with eosinophils and histopathological disease severity. Using the model of colonic eosinophilic inflammation and eotaxin-2$^{-/-}$ and eotaxin-1/-2$^{-/-}$ mice, we demonstrate a critical role for eotaxin-1 in eosinophil recruitment in the colon and a link between disease pathology and eosinophil infiltration. In situ hybridization and immunofluorescence analysis illuminated that eotaxin-1 was predominantly derived from intestinal macrophages in dextran sodium sulfate (DSS)-induced colitis; however analysis in pediatric UC revealed that eotaxin-1 expression was restricted to intestinal macrophages and the basolateral component on intestinal epithelial cells. These studies demonstrate an important link between activated intestinal macrophages, eotaxin-1, and eosinophil recruitment in pediatric UC.

Materials and Methods

Patient-based studies

Pediatric patients aged (5–18 years) were drawn from a consecutive sample of 124 individuals who were referred to the Cincinnati Children's Hospital Medical Center between April 2004 and November 2007. The study population was not part of a formal screening program, but it is representative of all clinical referrals to the IBD center. No patient had a history of IBD before colonic biopsy, and no patients were included who were referred for tertiary management. Of the 124 patients scheduled for diagnostic colonoscopy, 101 (81.5%) consented to participate in the study and underwent diagnostic evaluation. Colonic biopsy samples were collected and the diagnosis of UC was made using established clinical, radiological, and histological criteria. Patients with indeterminate colitis were excluded. No patient was receiving medications for the treatment of IBD at the time of biopsy. Of the 101 patients, 28 (27.7%) were diagnosed with CD and 13 (12.9%) with UC, and 60 (59.4%) were healthy controls. The first eight UC and 11 healthy controls were used in the gene chip array analysis. For UC patients, biopsies were taken from the ascending, descending, and rectosigmoid colon if affected and from the most proximal affected area otherwise. The pediatric ulcerative colitis clinical activity index was used as a measure of clinical severity of UC (28). The Montreal classification system was used to classify patients by age at diagnosis and by disease location and behavior (29). The study was approved by the Cincinnati Children's Hospital Medical Center (CCHMC) Institutional Review Board and the CCHMC General Clinical Research Center Scientific Advisory Committee.

Human colon biopsy histologic severity analysis

Paraffin-embedded, hematoxylin-stained colon biopsies were scored in a blinded manner by an experienced pediatric pathologist (E.B.) using the UC histologic index of severity (UCHIS). The UCHIS is a validated histologic score of inflammation for UC that accounts for the severity of acute and chronic inflammation (30).

Gene array analysis

Two colon biopsies from healthy controls and the most proximal affected areas for UC were obtained at the time of colonoscopy and immediately placed in RNAlater (Qiagen) at 4°C. Total RNA was isolated using the RNeasy Plus Mini Kit (Qiagen) and stored at −80°C. RNA samples were measured by the Agilent Bioanalyzer 2100 (Hewlett Packard) using the RNA

6000 Nano assay to confirm a 28S/18S ratio of 1.6 –2.0. RNA (100 ng) was amplified using TargetAmp 1-Round Aminoallyl-aRNA Amplification Kit 101 (Epicentre). The biotinylated cRNA was hybridized to Affymetrix GeneChip Human Genome HG-U133 Plus 2.0 arrays containing probes for ~22,634 transcripts. The images were captured using Affymetrix GeneChip Scanner 3000. GeneSpring software was used to analyze fold changes in gene expression between UC and healthy controls. Data were normalized to allow for array to array comparisons and differences between groups with a significance at the 0.05 level and mean fold change of 2 relative to healthy control samples. Principal component analysis was performed using the UC and healthy control results in GeneSpring. Ingenuity software (Ingenuity Systems) was used to group the differentially expressed genes into biologically relevant networks. The complete data set is available at the National Center for Biotechnology Information Gene Expression Omnibus site (www.ncbi.nlm.nih.gov/projects/geo) under accession number GSE10191.

Mice

Eotaxin-1/2 (sv129/C57BL/6), eotaxin-2-deficient (sv129/C57BL/6) (31), and eosinophil-deficient (PHIL) (C57BL/6) mice (32) and strain-matched wild-type (WT) (sv129/C57BL/6 and C57BL/6) mice (age 6 – 8 wk) were maintained under specific pathogen-free conditions and examined at age 6-to 8-wk. All mice were maintained in a specific pathogen-free vivarium, and animals were handled under Institutional Animal Care and Use Committee (Cincinnati Children's Hospital Medical Center)-approved protocols.

DSS induction of colonic injury

DSS used for the induction of experimental colitis (ICN Biomedical) was supplied with an average molecular mass of 41 kDa. It was used as a supplement in the drinking water of the mice for 7 days as a 2.5% (w/v) solution as we have previously described (33).

Eosinophil quantification

Segments of the GI tract including the colon were fixed with 4% paraformaldehyde/PBS, processed using standard histological techniques, and immunostained with antiserum against mouse major basic protein, as we have previously described (19).

Northern blot analysis

RNA was extracted from the colonic tissue using TRIzol reagent (Invitrogen) following the manufacturer's protocol. Twenty micrograms of total RNA was used for Northern blot analysis, as previously described (31).

Real-time PCR analysis

Human eotaxin-1, eotaxin-2 and eotaxin-3 mRNA were quantified by real-time PCR as previously described (34). In brief, the RNA samples (500 ng) were subjected to reverse transcription analysis using SuperScript II reverse transcriptase (Invitrogen) according to the manufacturer's instructions. Human eotaxin-1, eotaxin-2, and eotaxin-3 were quantified by real-time PCR using the iQ5 multicolor real-time PCR detection system (Bio-Rad Laboratories) with iQ5 software V2.0 and LightCycler FastStart DNA Master SYBR Green I. Primer sets were as follows: human eotaxin-3 (151 bp), 5′-AACTCCGAAACAATTGTACTCAGCTG-3′ and 5′-GTAACT CTGGGAGGAAACACCCTCTCC-3′; human eotaxin-2 (251 bp), 5′-CCATAGTAACCAGCCTTC-3′ and 5′-CAGGTTCTTCATGTACCTC-3′; human eotaxin-1 (425 bp), 5′-TGAAGCTTGGGCCAGCTTCTGTCCCAACC-3′ and 5′-GGTCGACTGGAGTTGGAGATTTTTGGTC-3′; and GAPDH (400 bp), 5′-TGGAAATCCCATCACCATCT-3′ and 5′-GTCTTC TGGGTGGCAGTGAT-3′. Results

were then normalized to GAPDH amplified from the same cDNA mix and expressed as fold induction compared with the controls.

In situ hybridization of mouse intestine

In situ hybridization was performed as we have previously described (35). In brief, the full-length murine eotaxin cDNA in plasmid Blue-script (36) was linearized by *Bam*HI or *Apa*I digestion, and antisense and sense RNA probes, respectively, were generated by T7 and T3 RNA polymerase (Riboprobe Gemini Core System II transcription kit; Promega). The radiolabeled ([α-^{35}S]thio-UTP) probes were reduced to an average length of 200 bases by controlled alkaline hydrolysis. The hybridized slides were washed under either high- or low-stringency conditions. For low stringency, the slides were washed for 60 min at 50°C in 50% formamide/5× SSC/20 mM DTT. This was followed by a 3-min RNase A digestion (20 μg/ml) at 37°C and 15-min washes in 2× SSC and 0.1× SSC (1× SSC = 0.15 M NaCl/0.015 M sodium citrate (pH 7.0)). For high stringency, the slides were washed at 65°C for 30 min in 50% formamide/2× SSC/10 mM DTT, rinsed three times in 500 mM NaCl/10 mM Tris · HCl (pH 7.5)/5 mM EDTA, digested with RNase A for 30 min at 37°C, and rinsed in fresh buffer. The high-stringency wash was repeated and then followed by two 15-min washes at room temperature, one in 2× SSC and one in 0.1× SSC/1 mM DTT. Autoradiography was performed for 14 –28 days at 4°C. The specificity of the hybridization was established by using a sense probe, which did not hybridize above background levels observed with the antisense probe. Sections from both wild-type controls and DSS-treated mice were hybridized and autoradiographed in triplicate under identical conditions.

Histological examination of mouse intestine

Colons were stained with H&E and examined and histologically scored by light microscopy as previous described (37). Colonic inflammation was evaluated in a blind manner by estimating the following: 1) percentage of involved area; 2) amount of follicles; 3) edema; 4) erosion/ulceration; 5) crypt loss; 6) infiltration of polymorphonuclear cells; and 7) infiltration of mononuclear cells. The percentage of area involved, erosion/ulceration, and the crypt loss were scored on a scale ranging from 0 to 4 as follows: 0, normal; 1, <10%; 2, 10 –25%; 3, 25–50%; and 4, >50%. Follicle aggregates were counted and scored as follows: 0, zero to one follicle; 1, two to three follicles; 2, four to five follicles; and 3, six follicles or more. The severity of the other parameters was scored on a scale from 0 to 3 as follows: 0, absent; 1, weak; 2, moderate; and 3, severe. All scores on the individual parameters together could result in a total score ranging from 0 to 24.

FACS analysis

Single cell suspensions from indicated organs were washed with FACS buffer (PBS/1% FCS) and incubated with combinations of the following Abs: PE anti-mouse F4/80 (clone CI:A3-1; Serotec) and PE-Cy7 anti-mouse CD11b (clone M1/70; BD Pharmingen). The following Abs were used as appropriate isotype controls; PE rat IgG2a (clone 53-6.7; BD Pharmingen) and PE-Cy7 rat IgG2a (clone R35-95; BD Pharmingen). Cells were analyzed on FACSCalibur (BD Immunocytometry Systems) and analysis was performed using Flow Jo software (Tree Star).

Intestinal macrophage purification

Macrophage/monocyte populations from colon were isolated by adherence as previously described (38). In brief, the colon segment of the GI tract was removed and flushed with 20 ml of Ca^{2+}- and Mg^{2+}-free HBSS (CMF-HBSS). The colon was cut longitudinally, placed in CMF-HBSS containing 5 mM EDTA and 25 mM HEPES, and shaken vigorously at 4°C for 30 min. The tissue was cut into 1-cm segments and incubated in digestion buffer containing 40 mg/ml collagenase A (Roche Diagnostics) in RPMI 1640 for 60 min on a shaker at 37°C.

The tissue was vigorously vortexed every 10 min for 15 s. Following the 60-min incubation, the cell aggregates were dissociated by filtering thorough a 19.5-gauge needle and 70-μm filter and centrifuged at 1200 rpm for 10 min at 4°C. The supernatant was decanted and the cell pellet resuspended in RPMI 1640 and filtered through a 40-μm filter. The single cell suspension was prepared by Ficoll density gradient centrifugation and quantitated by trypan blue exclusion analysis. Colonic cells (1×10^6) were plated in a 24-well, round-bottom plate and incubated at 37°C for 2 h in 5% CO_2. The adherent cells were washed three times and maintained in RPMI 1640 plus 10% FCS at 37°C for 2 h in 5% CO_2. The supernatant was removed and analyzed for eotaxin-1 levels by ELISA as described by the manufacturer (R&D Systems). The adherent cells were analyzed for purity by immunofluorescence analysis using the rat anti-mouse Mac-3 Ab and >95% cells were Mac-3^+. Contaminating cells were identified as intestinal epithelial cells and fibroblasts by cell morphology.

Immunofluorescence microscopy

In brief, fixed frozen sections were fixed in 10% acetone for 10 min, rinsed in PBS and washed in 0.025% Triton X-100/PBS three times for 5 min. The slides were blocked with 3% goat serum/PBS for 1 h at room temperature and incubated with primary Abs as follows: mouse anti-human CD68 (clone PG-M1) (2 μg/ml) (DakoCytomation); affinity-purified rabbit anti-human eotaxin-1 anti-serum (1/50); rat anti-mouse F4/80 (clone BM8) (5 μg/ml); rat anti-mouse Mac-3 (clone M3/84; BD Pharmingen) (4 μg/ml); and goat anti-mouse eotaxin-1 polyclonal (15 μg/ml; R & D Systems) in 3% normal goat serum/PBS. Sections were incubated with isotype control alone in place of primary Ab as a negative control. After a 2-h incubation at room temperature, sections were washed with PBS and incubated with goat anti-rabbit Alexa Fluor 488, donkey anti-goat Alexa Fluor 594, or donkey anti-rat Alexa Fluor 488 (Invitrogen) for 60 min at room temperature. Slides were washed in PBS and counterstained with 4′,6-diamidino-2-phenylindole (DAPI) di-hydrochloride/Supermount G solution (Fluoromount-G). Images were captured using a Zeiss microscope fitted with Zeiss UPlanApo lenses (×10, ×20, and ×40 magnification) and an AxioCam MRc camera and analyzed with Axioviewer version 3.1 image analysis software (Carl Zeiss). Postacquisition processing (brightness, opacity, contrast, and color balance) was applied to the entire image and accurately reflects that of the original.

Anti-eosinophil peroxidase (EPO) immunohistochemistry analysis

Anti-EPO immunohistochemistry analysis was performed using an affinity-purified anti-human EPO mAb. In brief, Ag retrieval was performed on colonic sections using the DakoCytomation Target Retrieval Solution as described by the manufacturer. The slides were digested in proteinase K and blocked in DakoCytomation Dual endogenous blocking solution. Slides were washed and incubated with either Ab control (mouse IgG2a; 10 μg/ml) or affinity-purified anti-human EPO mAb (mouse anti-human EPO, isotype IgG; 10 μg/ml; generated by Dr. J. Lee; Mayo Clinic, Scottsdale, AZ). The EPO-positive signal was detected with the DakoCytomation LSAB-2 alkaline phosphatase system and developed with the alkaline phosphatase substrate Permanent Red chromogen and counterstained with Methyl Green.

Statistical analysis

Unless otherwise indicated, data are expressed as mean ± SE (SEM). Statistical significance comparing two groups was determined by the nonparametric Mann-Whitney *U* test. In experiments comparing multiple experimental groups, nonparametric one-way ANOVA analysis (Kruskal-Wallis test) was performed across all groups, with a post hoc comparison analysis (Dunnett Post test) to determine significance as compared with the control group. $p < 0.05$ was considered significant. Correlative analysis was performed using a Spearman rank order correlation coefficient analysis. All analyses were performed using Prism 4.0 software.

Results

Patient demographics

Patients were drawn from a consecutive sample of 124 individuals who were referred to the Cincinnati Children's Hospital Medical Center between April 2004 and November 2007. Of the 124 patients scheduled for diagnostic colonoscopy, 101 (81.5%) consented to participate in the study and underwent diagnostic evaluation. The patient demographics for the UC and control groups are described in Table I.

Eosinophil accumulation and degranulation in pediatric UC

Histological analysis of lesional rectosigmoid colonic mucosa from pediatric UC patients revealed a pronounced cellular infiltrate consisting of mononuclear cells, neutrophils, and eosinophils. In lesional regions of the lamina propria, an intense eosinophilic infiltrate was observed (Fig. 1*b*, *inset*). Eosinophils were predominantly localized in intense pockets within the lamina propria; however, eosinophils within the mucosal epithelium and also the intercryptic regions were identified (Fig. 1*b*, *inset)*. Quantification of eosinophils revealed a significant increase in rectosigmoid eosinophil levels in pediatric UC patients as compared with normal patients (Fig. 1*c*) (eosinophils/high powered field (hpf) expressed as mean with lower 95% confidence interval and upper 95% confidence interval in parentheses: 10.9 (6.2 and 15.6) vs 31.5 (19.8 and 43.2), normal vs pediatric UC patients; $p < 0.005$). We did not observe any significant increase in ascending or descending eosinophil levels in pediatric UC patients as compared with normal patients (data not shown). Immunohistochemical analysis with an eosinophil-specific anti-EPO Ab revealed EPO-positive staining of extracellular granules demonstrating extensive eosinophil degranulation (Fig. 1*e*, *inset*). Evaluation of the UC disease histological score index demonstrated a positive correlation between eosinophil levels and disease severity (Fig. 1*f*). These studies demonstrate elevated levels of activated eosinophils in pediatric UC and that the level of this cell positively correlates with disease severity.

Eotaxin-1, eotaxin-2, and eotaxin-3 expression in pediatric UC

To begin to delineate the molecular basis of eosinophil recruitment in pediatric UC, we subjected colonic biopsy samples from individual pediatric UC ($n = 8$) and normal patients ($n = 11$) to whole genome-wide transcript expression profile analysis using oligonucleotide-based DNA microarray chips. Of the 22,634 transcripts represented on these microarrays, 1,345 transcripts were differentially expressed in pediatric UC vs controls (online supplemental Fig. 1a and Table I).[4] Normal and UC groups were clustered into two distinct groups. We next performed principal component analysis based on genes that discriminate between the two distinct conditions (control and UC) and generated a three-dimensional plot (from an 888-dimensional plot) of the data (online supplemental Fig. 1b). Principal component analysis-based multidimensional scaling visualization separated samples in the controls and UC groups into a linearly separable gene expression data space. Principal component 1 accounted for 81.3% variance. These analyses confirmed that the UC transcriptome defined a unique genomic signature distinct from that observed in the healthy controls (online supplemental Fig. 1b). To delineate the molecular fingerprint of UC, the differentially regulated genes were assigned to functional groups based on classification by Gene Ontology (www.geneontology.org/) and references in the literature. The majority of genes fell into the following groups: lipid metabolism, molecular transport, host defense, innate immune responses, response to biotic and inflammatory stimulus, chemotaxis, cell proliferation, and tumor growth (online supplemental Table S1). Using the Ingenuity software application, we identified a highly

[4]The online version of this article contains supplemental material.

expressed biological network whose primary function is in host defense, innate immune activation, and regulation of leukocyte recruitment (online supplemental Fig. 1c). This network included Toll receptors (TLR2, TLR7, and TLR8), innate signaling molecules (NOD2 and TWIST2; where NOD2 is nucleotide-binding oligomerization domain containing 2), proinflammatory cytokines and cytokine receptors (IL-1b, IL-18BP, IL-8RB, IL-10RA) and chemokines (CXCL2, CXCL3, CXCL9, CXCL10, CCL4, eotaxin-1, CCL19, CCL21, and IL-8) (online supplemental Fig. 1c).

Comparison of the transcript expression profile of pediatric UC patients to normal individuals revealed differential expression of eosinophil-specific chemokines including eotaxin-1 and eotaxin-2, but not eotaxin-3, in the colonic biopsy samples (Fig. 2*a*). Eotaxin-1 expression positively correlated with eosinophil levels within rectosigmoid biopsy samples of these patients (Fig. 2*b*). To confirm our whole genome-wide approach, we performed quantitative real-time PCR analysis and demonstrate a ~50-fold increase in eotaxin-1, a modest but not statistically significant increase in eotaxin-2 expression, and no change in eotaxin-3 mRNA expression in colonic biopsies from pediatric UC patients as compared with normal patients (Fig. 2, *c*–*e*).

Eosinophils in experimental DSS-induced colonic injury

To delineate the role of the eotaxins in colonic eosinophilic inflammation, we used a dextran sodium sulfate (DSS)-induced colonic injury model. Quantification of the colon eosinophil levels and histological score index from WT mice following DSS administration revealed a positive correlation between eosinophil levels and disease severity (day 8) (Fig. 3*a*). To definitively test the role of eosinophils in the histopathology of DSS-induced colonic injury, we used transgenic mice devoid of eosinophils (PHIL mice) (32). DSS treatment of littermate WT mice induced histopathologic damage to the colon, including a pronounced inflammatory infiltrate, crypt loss, and epithelial erosion (Fig. 3, *b* and *d*). Administration of DSS to PHIL mice revealed that the DSS-induced damage was significantly reduced in PHIL mice compared with WT mice (Fig. 3, *b* and *e*; $p < 0.01$). Consistent with this observation, the reduction in colon length, a classical feature of both DSS-induced colonic injury and IBD, was also reduced compared with WT mice (Fig. 3*c*). Collectively, these studies confirm eosinophil involvement in the histopathologic response in DSS-induced colonic injury.

Eosinophil-selective chemokines eotaxin-1 and eotaxin-2 in DSS-induced colonic injury

To assess the involvement of the eotaxins in eosinophil recruitment into the colon in DSS-induced colonic injury, we performed Northern blot analysis probing for eotaxin-1 and eotaxin-2 mRNA expression. We demonstrate that eotaxin-1 and eotaxin-2 are constitutively expressed at baseline (Fig. 4*a*). Furthermore, we show that administration of DSS significantly up-regulated eotaxin-1 and eotaxin-2 mRNA expression (Fig. 4*a*; *bottom panel*). The DSS-induced increase in eotaxin-1 and eotaxin-2 mRNA expression correlated with eosinophil recruitment into the colon (Fig. 4*a*, *upper panel*). Administration of DSS to strain- and aged-matched WT, eotaxin-2$^{-/-}$, and eotaxin-1/-2 deficient (eotaxin-1/-2$^{-/-}$) mice demonstrated that eotaxin-1 is central in the recruitment of eosinophils into the colon during DSS-induced colonic injury (Fig. 4*b*).

Cellular source of eotaxin-1 in DSS-induced colitis

To localize the cellular source of eotaxin-1 in DSS-induced colonic injury, we performed in situ hybridization analysis using eotaxin-1 anti-sense probe (Fig. 5). Darkfield analysis demonstrates that the eotaxin-1 anti-sense probe yielded a strong signal in DSS-treated mice (day 6) as compared with controls (Fig. 5, *b* and *d*). Darkfield microscopy revealed that the signal was concentrated within the lamina propria and mucosa of the colon of DSS-treated mice as compared with the control mice (Fig. 5, *b* and *d*). Specificity of the hybridization was

established by using a sense probe, which did not hybridize above background levels observed with the anti-sense probe (results not shown). High magnification demonstrates that the signal is predominantly localized to mononuclear cells beneath the crypt and also within the submucosa (Fig. 5*e*; arrowheads). To identify the eotaxin-1 mRNA-positive cells we performed flow cytometry analysis on partially purified colonic lamina propria cells from WT mice administered DSS for 6 days (maximal eotaxin-1 mRNA expression; Fig. 4*a*). Initially, we examined macrophages ($CD11b^+$ and $F4/80^+$ cells) because previous clinical and experimental studies have demonstrated that macrophages play an important role in the augmentation of the inflammatory response in chemical-induced colitis and IBD (39). Colonic lamina propria macrophages were identified by FSC^{high}, SSC^{high}, $CD11b^+$, and $F4/80^+$ cells (Fig. 6, *a* and *b*; where FSC is forward scatter and SSC is side scatter). Four or five days of DSS treatment induced no increase in the percentage of $CD11b^+/F4/80^+$ cells in the lamina propria of the colon of DSS-treated mice as compared with vehicle-treated mice (Fig. 6*c*). In contrast, on day 6 we observed a significant increase (~4-fold) in double positive $CD11b/F4/80^+$ cells (Fig. 6*c*). To examine whether intestinal macrophages were positive for eotaxin-1, intestinal macrophages were purified by adherence and eotaxin-1 levels were quantitated. Levels of eotaxin-1 within the intestinal macrophage lysates were significantly increased in DSS-treated mice as compared with vehicle-treated animals (Fig. 6*d*). To confirm eotaxin-1 expression by adherent macrophages, we performed two-color immunofluorescence analysis using Abs against eotaxin-1 and the macrophage marker (Mac-3). Notably, we demonstrate the colocalization of a Mac-3/eotaxin-1-positive signal (Fig. 6*e*). To confirm macrophage-derived eotaxin-1 in vivo, we performed two-color immunofluorescence analysis on colonic tissue from DSS-treated mice. We demonstrate colocalization of F4/80 and eotaxin-1 (Fig. 7, *upper panels*, yellow arrows) in the colons of mice treated with DSS (day 6), confirming macrophage derived eotaxin-1 expression in vivo. Notably, in our ex vivo or colonic tissue analysis, we show that not all macrophage ($Mac\text{-}3^+$ or $F4/80^+$) cells within the colon were eotaxin-1-positive (Fig. 6*e* and Fig. 7, *upper panels*, white arrows), suggesting that a subset of intestinal macrophages express eotaxin-1.

Following our experimental analysis demonstrating eotaxin-1 expression in intestinal macrophages in DSS-induced colonic injury, we next wanted to assess whether eotaxin-1 was expressed by macrophages in pediatric UC. We performed two-color immunofluorescence analysis (eotaxin-1, CD68, and DAPI) on lesional colonic biopsy samples from pediatric UC patients. We demonstrate colocalization of eotaxin-1^+CD68^+ cells in the colon of pediatric UC patients. Eotaxin-1^+CD68^+ cells were observed throughout the lamina propria (Fig. 7, *lower panels*). Notably, eotaxin-1 was also localized to the basolateral compartment of the intestinal epithelium within the colons of pediatric UC patients (Fig. 7, *lower panel*, white arrows). Collectively, these studies demonstrate that intestinal macrophages and epithelial cells express eotaxin-1 in pediatric UC.

Discussion

Previous investigations have demonstrated a link between elevated levels of eosinophils, eosinophil activation, and adult IBD. However, there have been conflicting data regarding the individual contribution of the eosinophil-selective chemokines eotaxin-1 and eotaxin-2 in eosinophil recruitment in IBD. In the present study we demonstrate the following: 1) that eosinophil numbers are elevated in pediatric UC and that their level correlates with disease severity; 2) eotaxin-1 and not eotaxin-2 or eotaxin-3 is up-regulated in lesional colonic biopsy samples of pediatric UC patients; and 3) eotaxin-1 mRNA expression correlates with colonic eosinophil levels in pediatric UC. Using a chemical-induced colonic injury model, we define that eotaxin-1, and not eotaxin-2, is critical for eosinophil recruitment and that eotaxin-1 is predominantly derived from intestinal macrophages. Consistent with our experimental

analysis, we show that eotaxin-1 is predominantly expressed by intestinal macrophages; however, we also identify intestinal epithelial cells as a source of eotaxin-1 in pediatric UC.

Previous clinical studies have demonstrated elevated levels of eosinophils in adult CD and UC and that the level of this leukocyte correlated with disease severity and GI dysfunction (2,6, 7,40,41). However, relatively few clinicopathologic studies have examined eosinophil involvement in pediatric UC. We now provide data demonstrating increased rectosigmoid eosinophil levels in the absence of significant increases in either the ascending or descending colon in pediatric UC. Increased eosinophils in adult UC have been shown to be localized to cecal and lesional large bowel biopsy samples (4,26,40) and are considered to be a negative prognostic indicator for UC. Notably, while eosinophils are not a component of the established UCHIS (30), we demonstrate a correlation between rectosigmoid eosinophil levels and disease severity. Interestingly, clinical severity of pediatric-onset UC is often greater in comparison to adult-onset disease (42,43). Approximately 60% of pediatric patients have moderate-to-severe disease at diagnosis and almost 80 –90% have pancolitis whereas 24% have pancolitis or 33% extensive colitis in adult onset (42–44). Furthermore, a higher rate of corticosteroid dependence (45%) in children as compared with adults as been observed (45). The increased clinical severity and steroid dependency may be attributable to a number of factors, including differences in disease immunopathogenesis and intestinal location between children and adults (46). However it is interesting to speculate that rectosigmoid eosinophils may contribute to corticosteroid dependency in pediatric UC. Notably, Lampinen and colleagues have previously demonstrated no reduction in eosinophil chemotactic activity in perfusion fluids from adult UC patients following corticosteroid therapy (47).

The role of eosinophils in IBD, particularly UC, is not yet fully elucidated (48). We demonstrate extensive eosinophil degranulation in pediatric UC, suggesting a link between eosinophil degranulation and the development of intestinal pathology. This is consistent with previous clinical investigations providing ultrastructural evidence of eosinophil degranulation in adult IBD (49). Notably, we demonstrate the presence of extracellular EPO in colonic biopsies from UC patients. EPO catalyzes the oxidation of halides, pseudohalides, and nitrite to generate cytotoxic oxidants (3-bromotyrosine, 3-chlorotyrosine, and hypothiocyanite) and reactive nitrogen species (3-nitrotyrosine and peroxynitrite) that induce tissue damage and cell death (50). Using a DSS-induced model of experimental colitis, we have previously demonstrated that ablation of EPO enzymatic activity by gene targeting or drug antagonism attenuated DSS-induced pathology (51). We are currently assessing the contribution of EPO to the histopathology of pediatric UC.

Previous investigations have demonstrated elevated levels of serum eotaxin-1 in adult UC patients as compared with controls; however, an association between eotaxin-1 and colonic eosinophil levels has not yet been established (24,25). In the present study, we demonstrate increased expression of eotaxin-1 in colonic biopsy samples from pediatric UC patients. In addition, we show that expression of this chemokine positively correlated with eosinophil recruitment, demonstrating a direct link between eotaxin-1 and eosinophils in IBD. Previous genetic analyses have also demonstrated a link between adult UC and eotaxin-2. Allelic frequency of +179T→C and +275C→T of eotaxin-2 and genotype differences correlated with UC susceptibility (27). However, our analysis did not identify any difference in eotaxin-2 mRNA expression in pediatric UC, suggesting no role for eotaxin-2 in the recruitment of eosinophils in pediatric UC. Consistent with this observation, genetic deletion of eotaxin-2 had no effect on experimental DSS-induced colonic eosinophil inflammation. Collectively, these data and experimental analysis demonstrate an important role for eotaxin-1 in eosinophil recruitment into the colon.

We performed gene profiling analysis on pediatric UC patients at diagnosis and on normal patients and revealed a pediatric UC gene signature. The up-regulated genes possessed a broad range of functions primarily associated with cellular growth and proliferation, innate immune defense mechanisms, lipid and carbohydrate metabolism, and molecular transport. Innate immune genes up-regulated in UC consisted of an abundance of genes involved in leukocyte recruitment and activation (*CXCL1*, *CXCL2*, *CXCL3*, *CXCL5*, *CXCL6*, *CXCL9*, *CXCL10*, *CXCL11*, *eotaxin-1*, *and CXCL8/IL-8*). Elevated levels of CXCL8/IL-8, CXCL9/MIG, and CXL10/IP-10 mRNA and protein have previously been demonstrated in UC (52–54). Furthermore, experimental analyses have demonstrated a key role for these chemokines in DSS-induced colonic intestinal inflammation and disease pathology (55–57). IL-8, CXCL9, and CXCL10 are primarily involved in the regulation of macrophage, neutrophil, and T cell trafficking. Collectively, these network analyses reveal a link between macrophages, neutrophils, and T cells that is thought to play a pivotal role in the augmentation of the intestinal inflammatory response in IBD and the eotaxin-1/eosinophil pathway. Consistent with this notion, we demonstrate that eotaxin-1 is primarily secreted by macrophages.

Previous genome-wide array analysis in adult UC has demonstrated a significant increase in CXCL1, CXCL2, CXCL3, eotaxin-1, and IL-8, suggesting that there is up-regulation of common immune pathways between pediatric- and adult-onset UC gene signature (58). However, the majority of up-regulated networks in adult UC were associated with biosynthesis, metabolism, and electrolyte transport (58). In contrast, in our pediatric UC population a significant proportion of genes up-regulated were associated with immune response, immune and lymphatic system development, and function and immunological disease networks. One possible explanation for the predominance of immune networks in our studies is that our analysis was performed at diagnosis in the absence of therapy, whereas the previous study analyzed adult UC patients receiving therapy including aminosalicylates, antibiotics, steroids and immunomodulators (azathioprine, 6-mercaptopurine (6MP), or infliximab). Analysis of the UC gene signature in the absence of therapy will illuminate important gene networks involved in early stages of the immunopathophysiology of UC. Notably, we also observed altered expression of gene networks associated with cancer, cellular growth, and proliferation at diagnosis in our pediatric UC population (results not shown). UC is associated with an elevated risk for colorectal cancer (59). This would suggest activation of proliferative pathways associated with tumorigenesis and proliferation early in disease onset.

Immunofluorescence analysis of colonic biopsy samples from UC patients demonstrated eotaxin-1 expression by intestinal epithelial cells and $CD68^+$ macrophages. Notably, the eotaxin-1 signal from intestinal epithelial cells was restricted to the basolateral compartment. Consistent with this, we observed the accumulation of eosinophils between and beneath the intestinal epithelium. Previous studies with human intestinal epithelial cells have demonstrated *Cryptosporidium parvum*- and *Bacteroides fragilis*-induced basolateral expression of the CXC chemokines IL-8, and GROα(60,61). In both human and mouse studies we also demonstrated that macrophages are a primary source of eotaxin-1. Intestinal macrophage levels have been shown to be elevated in IBD and activation correlated with disease severity (62). Furthermore, previous immunohistochemistry analysis examining eotaxin-1 production in mucosal tissues derived from CD and UC identified a minor population of eotaxin-1-positive mononuclear inflammatory cells; however the cell type was not identified (26). Experimental studies using macrophage-deficient *op/op* mice have demonstrated a role for macrophages in *Nocardia brasiliensis* infection-induced eosinophil recruitment (63).

NF-κB-dependent signaling pathways are thought to be important in the orchestration of the intestinal inflammatory response associated with IBD. Furthermore, activated NF-κB has been localized to intestinal macrophages and epithelial cells from IBD patients (62). Eotaxin-1 promoter possesses STAT-6 and NF-κB regulatory elements in the promoter region (64).

Furthermore, eotaxin-1 expression in airway smooth muscle cells and epithelial cells has been shown to be regulated by NF-κB- and STAT-6-dependent pathways (64). It is tempting to speculate that NF-κB activation of intestinal epithelial cells and macrophages drives eotaxin-1 expression and subsequent eosinophil recruitment in experimental colitis and pediatric UC. Consistent with this hypothesis, blockade of NF-κB signaling by decoy oligonucleotides attenuates murine Th1- and Th2-mediated IBD (65).

In conclusion, we demonstrate a direct link between eotaxin-1 and intestinal macrophages in eosinophilic inflammation of the colon in experimental models and pediatric UC. Further, we demonstrate an important role for eotaxin-1 in the recruitment of eosinophils into the colon during IBD and show that eosinophils may have a role in the disease pathogenesis. Because pediatric onset UC is often more extensive and severe as compared with adult UC and possesses a higher rate of steroid dependency, delineation of the inflammatory pathways involved in disease pathogenesis is critical as emerging therapeutic approaches are introduced into treatment. Our studies provide strong rationale for the usage of therapeutic approaches targeting eosinophils or the eotaxin-1 pathway (eotaxin-1/CCR3) for pediatric UC.

Supplementary Material

Refer to Web version on PubMed Central for supplementary material.

Acknowledgments

We thank other members of the Division of Allergy and Immunology and Gastroenterology, Hepatology, and Nutrition, Cincinnati Children's Hospital Medical Center for insightful conversations. We also thank Cheryl Protheroe for histopathology expertise, Melissa Mingler and Melissa McBride for animal husbandry and maintenance of mouse colony, and Dr. Fabiana Machado for assistance with the immunofluorescence analysis.

References

1. Bouma G, Strober W. The immunological and genetic basis of inflammatory bowel disease. Nat Rev Immunol 2003;3:521–533. [PubMed: 12876555]
2. Walsh RE, Gaginella TS. The eosinophil in inflammatory bowel disease. Scand J Gastrorenterol 1991;26:1217–1224.
3. Desreumaux P, Nutten S, Colombel JF. Activated eosinophils in inflammatory bowel disease: do they matter? Am J Gastroenterol 1999;94:3396 –3398. [PubMed: 10606287]
4. Nishitani H, Okabayashi M, Satomi M, Shimoyama T, Dohi Y. Infiltration of peroxidase-producing eosinophils into the lamina propria of patients with ulcerative colitis. J Gastroenterol 1998;33:189 –195. [PubMed: 9605947]
5. Rothenberg ME, Hogan SP. The eosinophil. Annu Rev Immunol 2006;24:147–174. [PubMed: 16551246]
6. Raab Y, Fredens K, Gerdin B, Hallgren R. Eosinophil activation in ulcerative colitis: studies on mucosal release and localization of eosinophil granule constituents. Dig Dis Sci 1998;43:1061–1070. [PubMed: 9590423]
7. Carlson M, Raab Y, Peterson C, Hallgren R, Venge P. Increased intraluminal release of eosinophil granule proteins EPO, ECP, EPX, and cytokines in ulcerative colitis and proctitis in segmental perfusion. Am J Gastroenterol 1999;94:1876 –1883. [PubMed: 10406252]
8. Moser R, Fehr J, Bruijnzeel PL. IL-4 controls the selective endothelium-driven transmigration of eosinophils from allergic individuals. J Immunol 1992;149:1432–1438. [PubMed: 1354235]
9. Sher A, Coffman RL, Hieny S, Cheever AW. Ablation of eosinophil and IgE responses with anti-IL-5 or anti-IL-4 antibodies fails to affect immunity against *Schistosoma mansoni* in the mouse. J Immunol 1990;145:3911–3916. [PubMed: 2123226]

10. Horie S, Okubo Y, Hossain M, Sato E, Nomura H, Koyama S, Suzuki J, Isobe M, Sekiguchi M. Interleukin-13 but not interleukin-4 prolongs eosinophil survival and induces eosinophil chemotaxis. Intern Med 1997;36:179 –185. [PubMed: 9144009]

11. Bochner BS, Schleimer RP. The role of adhesion molecules in human eosinophil and basophil recruitment. J Allergy Clin Immunol 1994;94:427– 438. [PubMed: 8083447]

12. Zimmermann N, Hershey GK, Foster PS, Rothenberg ME. Chemokines in asthma: cooperative interaction between chemokines and IL-13. J Allergy Clin Immunol 2003;111:227–242. [PubMed: 12589338]

13. Zhu Z, Zheng T, Homer RJ, Kim YK, Chen NY, Cohn L, Hamid Q, Elias JA. Acidic mammalian chitinase in asthmatic Th2 inflammation and IL-13 pathway activation. Science 2004;304:1678 –1682. [PubMed: 15192232]

14. Rankin SM, Conroy DM, Williams TJ. Eotaxin and eosinophil recruitment: implications for human disease. Mol Med Today 2000;6:20 –27. [PubMed: 10637571]

15. Collins PD, Marleau S, Griffiths-Johnson DA, Jose PJ, Williams TJ. Cooperation between interleukin-5 and the chemokine eotaxin to induce eosinophil accumulation in vivo. J Exp Med 1995;182:1169 –1174. [PubMed: 7561691]

16. Flood-Page P, Phipps S, Menzies-Gow A, Ong YE, Kay AB. Effect of intravenous administration of an anti-IL-5 (mepolizumab) on allergen-induced tissue eosinophilia, the late-phase allergic reaction and the expression of a marker of repair/remodeling in human atopic subjects. J Allergy Clin Immunol 2003;111:S261.

17. Hogan SP, Koskinen A, Foster PS. Interleukin-5 and eosinophils induce airway damage and bronchial hyperreactivity during allergic airway inflammation in BALB/c mice. Immunol Cell Biol 1997;75:284 –288. [PubMed: 9243294]

18. Foster P, Hogan S, Ramsay A, Matthaei K, Young I. Interleukin-5 deficiency abolishes eosinophilia, airway hyperreactivity and lung damage in mouse asthma model. J Exp Med 1996;183:195–201. [PubMed: 8551223]

19. Forbes E V, Smart E, D'Aprile A, Henry P, Yang M, Matthaei KI, Rothenberg ME, Foster PS, Hogan SP. T helper-2 immunity regulates bronchial hyperresponsiveness in eosinophil-associated gastrointestinal disease in mice. Gastroenterology 2004;127:105–118. [PubMed: 15236177]

20. Gurish MF, Humbles A, Tao H, Finkelstein S, Boyce JA, Gerard C, Friend DS, Austen KF. CCR3 is required for tissue eosinophilia and larval cytotoxicity after infection with *Trichinella spiralis*. J Immunol 2002;168:5730 –5736. [PubMed: 12023373]

21. Rothenberg ME, MacLean JA, Pearlman E, Luster AD, Leder P. Targeted disruption of the chemokine eotaxin partially reduces antigen-induced tissue eosinophilia. J Exp Med 1997;185:785–790. [PubMed: 9034156]

22. Pope SM, Fulkerson PC, Blanchard C, Akei HS, Nikolaidis NM, Zimmermann N, Molkentin JD, Rothenberg ME. Identification of a cooperative mechanism involving interleukin-13 and eotaxin-2 in experimental allergic lung inflammation. J Biol Chem 2005;280:13952–13961. [PubMed: 15647285]

23. Gonzalo JA, Lloyd CM, Wen D, Albar JP, Wells TN, Proudfoot A, Martinez AC, Dorf M, Bjerke T, Coyle AJ, Gutierrez-Ramos JC. The coordinated action of CC chemokines in the lung orchestrates allergic inflammation and airway hyperresponsiveness. J Exp Med 1998;188:157–167. [PubMed: 9653092]

24. Chen W, Paulus B, Shu D, Wilson I, Chadwick V. Increased serum levels of eotaxin in patients with inflammatory bowel disease. Scand J Gastroenterol 2001;36:515–520. [PubMed: 11346206]

25. Mir A, Minguez M, Tatay J, Pascual I, Pena A, Sanchiz V, Almela P, Mora F, Benages A. Elevated serum eotaxin levels in patients with inflammatory bowel disease. Am J Gastroenterol 2002;97:1452–1457. [PubMed: 12094864]

26. Jeziorska M, Haboubi N, Schofield P, Woolley DE. Distribution and activation of eosinophils in inflammatory bowel disease using an improved immunohistochemical technique. J Pathol 2001;194:484 – 492. [PubMed: 11523058]

27. Park Y, Choi S, Lee SC, Kim KP, Chae SC, Chung HL. The association of eotaxin-2 and eotaxin-3 gene polymorphisms in a Korean population with ulcerative colitis. Exp Mol Med 2005;37:553–558. [PubMed: 16391516]

28. Turner D, Walsh CM, Benchimol EI, Mann EH, Thomas KE, Chow C, McLernon RA, Walters TD, Steinhart AH, Griffiths AM. Severe paediatric ulcerative colitis: incidence, outcomes, and optimal timing for second line therapy. Gut 2007;57:331–338. [PubMed: 17981888]
29. Satsangi J, Silverberg MS, Vermeire S, Colombel JF. The Montreal classification of inflammatory bowel disease: controversies, consensus, and implications. Gut 2006;55:749 –753. [PubMed: 16698746]
30. Rutter M, Saunders B, Wilkinson K, Rumbles S, Schofield G, Kamm M, Williams C, Price A, Talbot I, Forbes A. Severity of inflammation is a risk factor for colorectal neoplasia in ulcerative colitis. Gastroenterology 2004;126:451– 459. [PubMed: 14762782]
31. Pope SM, Zimmermann N, Stringer KF, Karow ML, Rothenberg ME. The eotaxin chemokines and CCR3 are fundamental regulators of allergen-induced pulmonary eosinophilia. J Immunol 2005;175:5341–5350. [PubMed: 16210640]
32. Lee JJ, Dimina D, Macias MP, Ochkur SI, McGarry MP, O'Neill KR, Protheroe C, Pero R, Nguyen T, Cormier SA, et al. Defining a link with asthma in mice congenitally deficient in eosinophils. Science 2004;305:1773–1776. [PubMed: 15375267]
33. Hogan SP, Mishra A, Brandt EB, Royalty MP, Pope SM, Zimmermann N, Foster PS, Rothenberg ME. A pathological function for eotaxin and eosinophils in eosinophilic gastrointestinal inflammation. Nat Immunol 2001;2:353–360. [PubMed: 11276207]
34. Blanchard C, Wang N, Stringer KF, Mishra A, Fulkerson PC, Abonia JP, Jameson SC, Kirby C, Konikoff MR, Collins MH, et al. Eotaxin-3 and a uniquely conserved gene-expression profile in eosinophilic esophagitis. J Clin Invest 2006;116:536 –547. [PubMed: 16453027]
35. Matthews AN, Friend DS, Zimmermann N, Sarafi MN, Luster AD, Pearlman E, Wert SE, Rothenberg ME. Eotaxin is required for the baseline level of tissue eosinophils. Proc Natl Acad Sci USA 1998;95:6273– 6278. [PubMed: 9600955]
36. Rothenberg M, Luster AD, Leder P. Murine eotaxin: an eosinophil chemoattractant inducible in endothelial cells and in interleukin 4-induced tumour suppression. Proc Natl Acad Sci USA 1995;92:8960 – 8964. [PubMed: 7568052]
37. Ten Hove T, Drillenburg P, Wijnholds J, Ate Velde A, van Deventer SJ. Differential susceptibility of multidrug resistance protein-1 deficient mice to DSS and TNBS-induced colitis. Dig Dis Sci 2002;47:2056 –2063. [PubMed: 12353855]
38. Crocker PR, Gordon S. Properties and distribution of a lectin-like hemagglutinin differentially expressed by murine stromal tissue macrophages. J Exp Med 1986;164:1862–1875. [PubMed: 3783087]
39. Schenk M, Bouchon A, Seibold F, Mueller C. TREM-1-expressing intestinal macrophages crucially amplify chronic inflammation in experimental colitis and inflammatory bowel diseases. J Clin Invest 2007;117:3097–3106. [PubMed: 17853946]
40. Bischoff SC, Mayer J, Nguyen QT, Stolte M, Manns MP. Immunohistological assessment of intestinal eosinophil activation in patients with eosinophilic gastroenteritis and inflammatory bowel disease. Am J Gastroenterol 1999;94:3521–3529. [PubMed: 10606314]
41. Carvalho AT, Elia CC, de Souza HS, Elias PR, Pontes EL, Lukashok HP, de Freitas FC, Lapa e Silva JR. Immunohistochemical study of intestinal eosinophils in inflammatory bowel disease. J Clin Gastroenterol 2003;36:120 –125. [PubMed: 12544193]
42. Hyams JS, Davis P, Grancher K, Lerer T, Justinich CJ, Markowitz J. Clinical outcome of ulcerative colitis in children. J Pediatr 1996;129:81– 88. [PubMed: 8757566]
43. Kugathasan S, Judd RH, Hoffmann RG, Heikenen J, Telega G, Khan F, Weisdorf-Schindele S, San Pablo W Jr, Perrault J, Park R, et al. Epidemiologic and clinical characteristics of children with newly diagnosed inflammatory bowel disease in Wisconsin: a statewide population-based study. J Pediatr 2003;143:525–531. [PubMed: 14571234]
44. Henriksen M, Jahnsen J, Lygren I, Sauar J, Kjellevold O, Schulz T, Vatn MH, Moum B. Ulcerative colitis and clinical course: results of a 5-year population-based follow-up study (the IBSEN study). Inflamm Bowel Dis 2006;12:543–550. [PubMed: 16804390]
45. Faubion WA Jr, Loftus EV Jr, Harmsen WS, Zinsmeister AR, Sandborn WJ. The natural history of corticosteroid therapy for inflammatory bowel disease: a population-based study. Gastroenterology 2001;121:255–260. [PubMed: 11487534]

46. Robert ME, Skacel M, Ullman T, Bernstein CN, Easley K, Goldblum JR. Patterns of colonic involvement at initial presentation in ulcerative colitis: a retrospective study of 46 newly diagnosed cases. Am J Clin Pathol 2004;122:94 –99. [PubMed: 15272536]
47. Lampinen M, Carlson M, Sangfelt P, Taha Y, Thorn M, Loof L, Raab Y, Venge P. IL-5 and TNF-α participate in recruitment of eosinophils to intestinal mucosa in ulcerative colitis. Dig Dis Sci 2001;46:2004 –2009. [PubMed: 11575456]
48. Miner PB Jr. Seeing red in inflammatory bowl disease: the eosinophil at center stage? Inflamm Bowel Dis 2004;10:329 –330. [PubMed: 15290934]
49. Dvorak AM. Ultrastructural evidence for release of major basic protein-containing crystalline cores of eosinophil granules in vivo: cytotoxic potential in Crohn's disease. J Immunol 1980;125:460 –462. [PubMed: 6155407]
50. MacPherson JC, Comhair SA, Erzurum SC, Klein DF, Lipscomb MF, Kavuru MS, Samoszuk MK, Hazen SL. Eosinophils are a major source of nitric oxide-derived oxidants in severe asthma: characterization of pathways available to eosinophils for generating reactive nitrogen species. J Immunol 2001;166:5763–5772. [PubMed: 11313420]
51. Forbes E, Murase T, Yang M, Matthaei KI, Lee JJ, Lee NA, Foster PS, Hogan SP. Immunopathogenesis of experimental ulcerative colitis is mediated by eosinophil peroxidase. J Immunol 2004;172:5664 –5675. [PubMed: 15100311]
52. Katsuta T, Lim C, Shimoda K, Shibuta K, Mitra P, Banner BF, Mori M, Barnard GF. Interleukin-8 and SDF1-α mRNA expression in colonic biopsies from patients with inflammatory bowel disease. Am J Gastroenterol 2000;95:3157–3164. [PubMed: 11095335]
53. Banks C, Bateman A, Payne R, Johnson P, Sheron N. Chemokine expression in IBD: mucosal chemokine expression is unselectively increased in both ulcerative colitis and Crohn's disease. J Pathol 2003;199:28 –35. [PubMed: 12474223]
54. Egesten A, Eliasson M, Olin AI, Erjefalt JS, Bjartell A, Sangfelt P, Carlson M. The proinflammatory CXC-chemokines GRO-α/CXCL1 and MIG/CXCL9 are concomitantly expressed in ulcerative colitis and decrease during treatment with topical corticosteroids. Int J Colorectal Dis 2007;22:1421–1427. [PubMed: 17703315]
55. Berrebi D, Languepin J, Ferkdadji L, Foussat A, De Lagausie P, Paris R, Emilie D, Mougenot JF, Cezard JP, Navarro J, Peuchmaur M. Cytokines, chemokine receptors, and homing molecule distribution in the rectum and stomach of pediatric patients with ulcerative colitis. J Pediatr Gastroenterol Nutr 2003;37:300 –308. [PubMed: 12960653]
56. Papadakis KA, Prehn J, Zhu D, Landers C, Gaiennie J, Fleshner P, Targan SR. Expression and regulation of the chemokine receptor CXCR3 on lymphocytes from normal and inflammatory bowel disease mucosa. Inflamm Bowel Dis 2004;10:778 –788. [PubMed: 15626897]
57. Sasaki S, Yoneyama H, Suzuki K, Suriki H, Aiba T, Watanabe S, Kawauchi Y, Kawachi H, Shimizu F, Matsushima K, et al. Blockade of CXCL10 protects mice from acute colitis and enhances crypt cell survival. Eur J Immunol 2002;32:3197–3205. [PubMed: 12555665]
58. Wu F, Dassopoulos T, Cope L, Maitra A, Brant SR, Harris ML, Bayless TM, Parmigiani G, Chakravarti S. Genome-wide gene expression differences in Crohn's disease and ulcerative colitis from endoscopic pinch biopsies: insights into distinctive pathogenesis. Inflamm Bowel Dis 2007;13:807– 821. [PubMed: 17262812]
59. Clevers HC. At the crossroads of inflammation and cancer. Cell 2004;118:671– 674. [PubMed: 15369667]
60. Laurent F, Eckmann L, Savidge TC, Morgan G, Theodos C, Naciri M, Kagnoff MF. Cryptosporidium parvum infection of human intestinal epithelial cells induces the polarized secretion of C-X-C chemokines. Infect Immun 1997;65:5067–5073. [PubMed: 9393797]
61. Kim JM, Oh YK, Kim YJ, Oh HB, Cho YJ. Polarized secretion of CXC chemokines by human intestinal epithelial cells in response to *Bacteroides fragilis* enterotoxin: NF-κB plays a major role in the regulation of IL-8 expression. Clin Exp Immunol 2001;123:421– 427. [PubMed: 11298129]
62. Rogler G, Brand K, Vogl D, Page S, Hofmeister R, Andus T, Knuechel R, Baeuerle PA, Scholmerich J, Gross V. Nuclear factor κB is activated in macrophages and epithelial cells of inflamed intestinal mucosa. Gastroenterology 1998;115:357–369. [PubMed: 9679041]

63. Voehringer D, Van Rooijen N, Locksley RM. Eosinophils develop in distinct stages and are recruited to peripheral sites by alternatively activated macrophages. J Leukocyte Biol 2007;81:1434 –1444. [PubMed: 17339609]

64. Matsukura S, Stellato C, Plitt JR, Bickel C, Miura K, Georas SN, Casolaro V, Schleimer RP. Activation of eotaxin gene transcription by NF-κB and STAT6 in human airway epithelial cells. J Immunol 1999;163:6876 – 6883. [PubMed: 10586089]

65. Fichtner-Feigl S I, Fuss J, Preiss JC, Strober W, Kitani A. Treatment of murine Th1- and Th2-mediated inflammatory bowel disease with NF-κB decoy oligonucleotides. J Clin Invest 2005;115:3057–3071. [PubMed: 16239967]

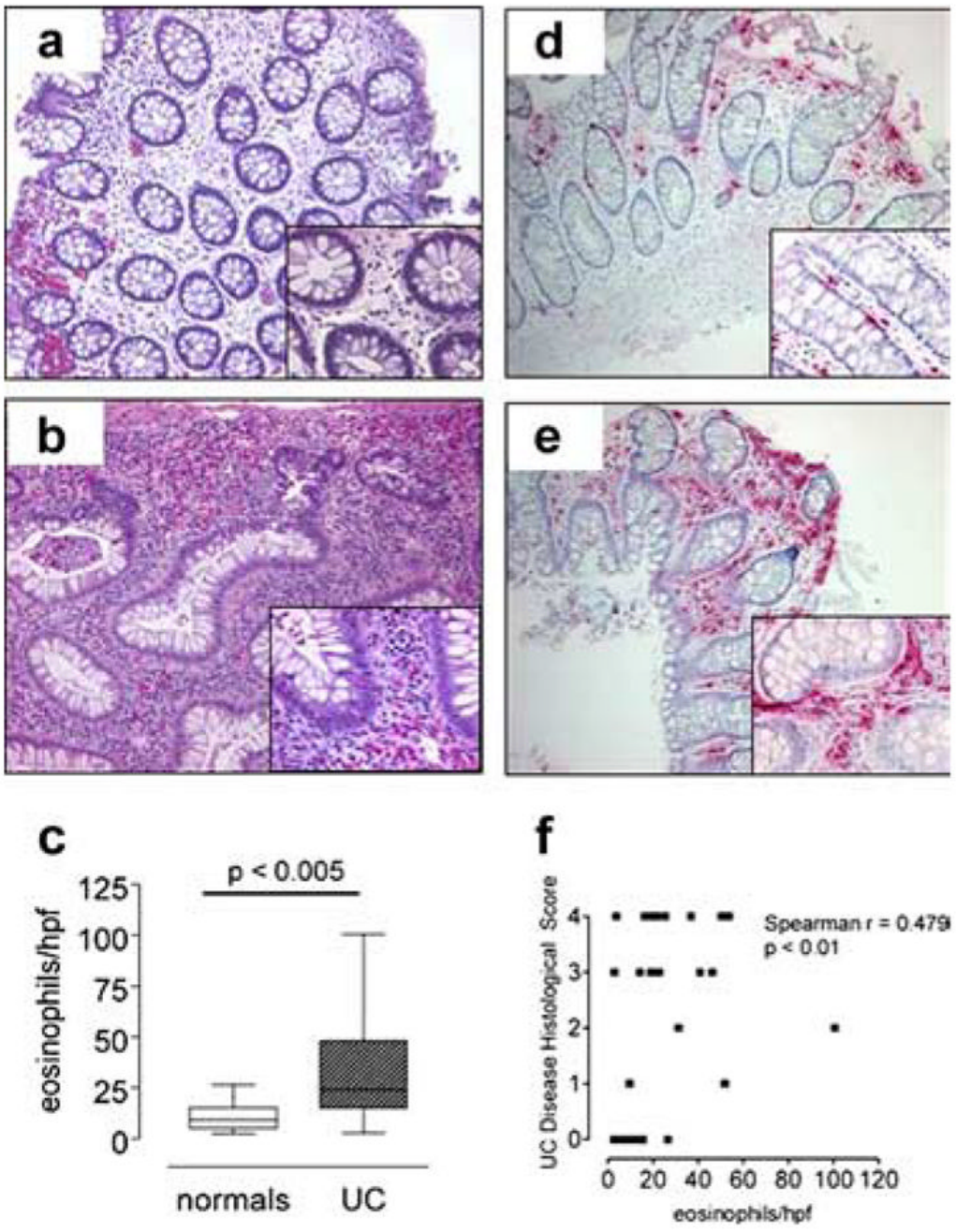

FIGURE 1.

Eosinophil levels and degranulation in pediatric UC. *a* and *b*, Representative H&E-stained rectosigmoid colonic biopsy samples from normal patients (normals) (*a*) and pediatric UC (*b*) patients. *c*, Eosinophil numbers/hpf in rectosigmoid colonic biopsy samples from normal and pediatric UC patients. *d* and *e*, Representative anti-EPO-immunostained rectosigmoid colonic biopsy samples from normal (*d*) and pediatric UC (*e*) patients. *f*, Correlation analysis of rectosigmoid eosinophil levels per hpf and disease histological score of rectosigmoid colonic biopsy samples from normal and pediatric patients. *c* is presented as the median ± 25% and 75% percentile (the *lower* and *upper quartiles*, respectively), and minimum and maximum limit (whiskers) (magnification: *a–d*, ×50; *insets*, ×200).

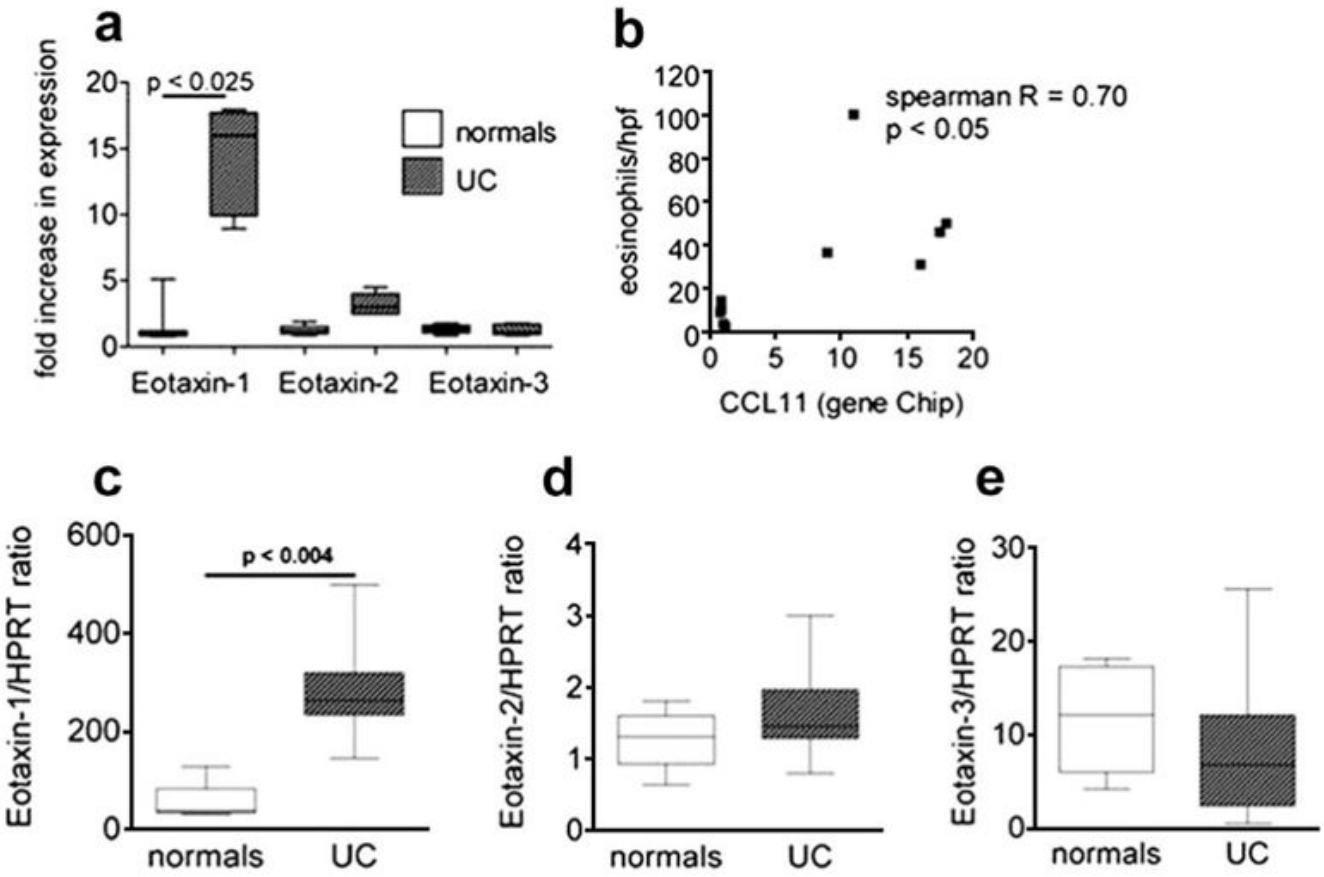

FIGURE 2.

Eotaxin subfamily expression in pediatric UC; eotaxin-1, -, and -3 expression in normal and UC patients. *a*, Eotaxin-1, -2, and -3 normalized expression in normal patients (normals) and UC patients by microarray analysis. *b*, Correlation between eosinophils/hpf of rectosigmoid colon and eotaxin-1 mRNA expression by microarray analysis (Spearman $R = 0.70$; $p < 0.05$). *c* and *d*, Quantitative analysis of *eotaxin-1*, *-2*, and *-3* mRNA levels in normal and UC patients using real-time PCR analysis. The levels of *eotaxin-1* (*c*), and *eotaxin-2* (*d*), and *eotaxin-3* (*e*) mRNA are shown. Each mRNA value is normalized to *HPRT* mRNA and is expressed as fold change. *a*, RNA from each patient was subjected to chip analysis using Affymetrix Human Genome U133 Plus 2.0 GeneChips. Data were normalized to allow for array to array comparisons, and differences between groups were detected in GeneSpring with a significance at the 0.05 level and mean fold change of 2 relative to healthy control samples. *c*–*e*, The graphs are standard box and whisker plots, providing median, 25th and 75th percentiles, and minimum and maximum limit (whiskers). The number of subjects was seven and five for normal and UC patients, respectively.

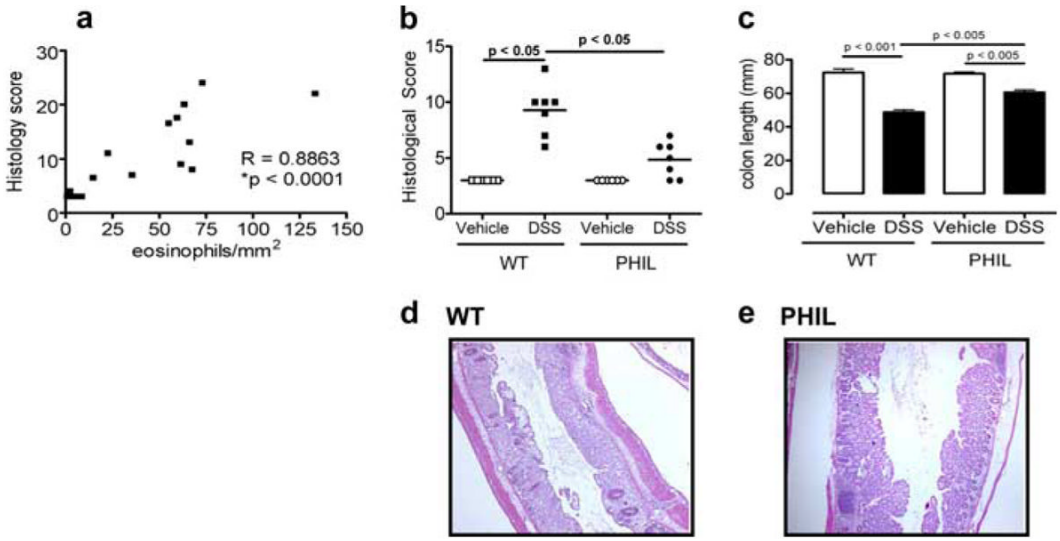

FIGURE 3.

Role of eosinophils in DSS-induced colitis. *a*, Correlation analysis between eosinophils/mm^2 in the colon vs the histological score of colons of WT mice treated with 2.5% DSS for 8 days. Histological score of colon (*b*) and colon length (*c*) of WT and eosinophil deficient (PHIL) mice treated with 2.5% DSS for 8 days. Representative photomicrographs of H&E-stained colonic sections from DSS-challenged WT (*d*) and PHIL (*e*) mice. *a*, Correlation analysis was performed by Spearman's correlation analysis. *b*, Each symbol represents one mouse and the line indicates the mean; *c*, Data represent mean ± SD. *d* and *e*, Magnification of photomicrographs is ×50.

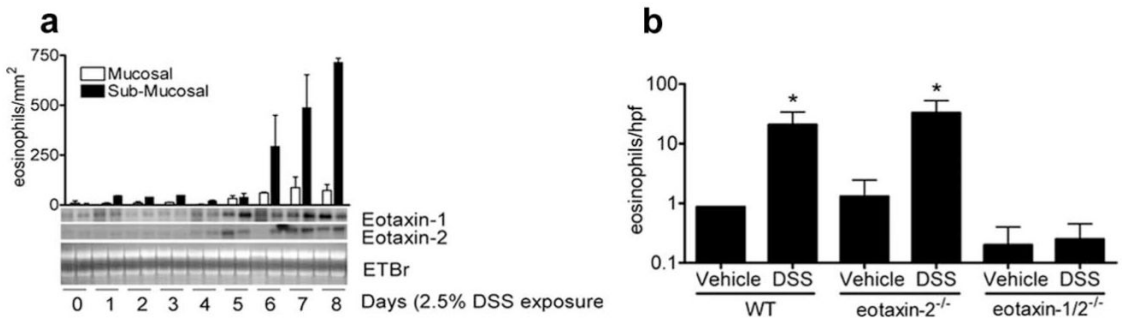

FIGURE 4.

Eosinophils and eotaxin-1 and -2 expression in DSS-induced colitis. *a*, Eosinophil/mm^2 in the mucosal and submucosal compartment (*upper panel*) and eotaxin-1 and eotaxin-2 mRNA expression (*lower panel*) in the colons of WT mice treated for 0 – 8 days with 2.5% DSS. Ethidium bromide (ETBr)-stained gel is shown to demonstrate RNA quality. Eotaxin-1 and -2 mRNA expression is shown as two mice per time point. *b*, Eosinophils/hpf in the submucosal of the colon of WT (SV129/Svev/C57BL/6) and eotaxin-2$^{-/-}$ and eotaxin-1/-2$^{-/-}$ mice treated with 2.5% DSS for 8 days. Data represent the mean ± SEM of 4 –5 random sections per mouse for 3– 6 mice per group; n = 2 experiments.

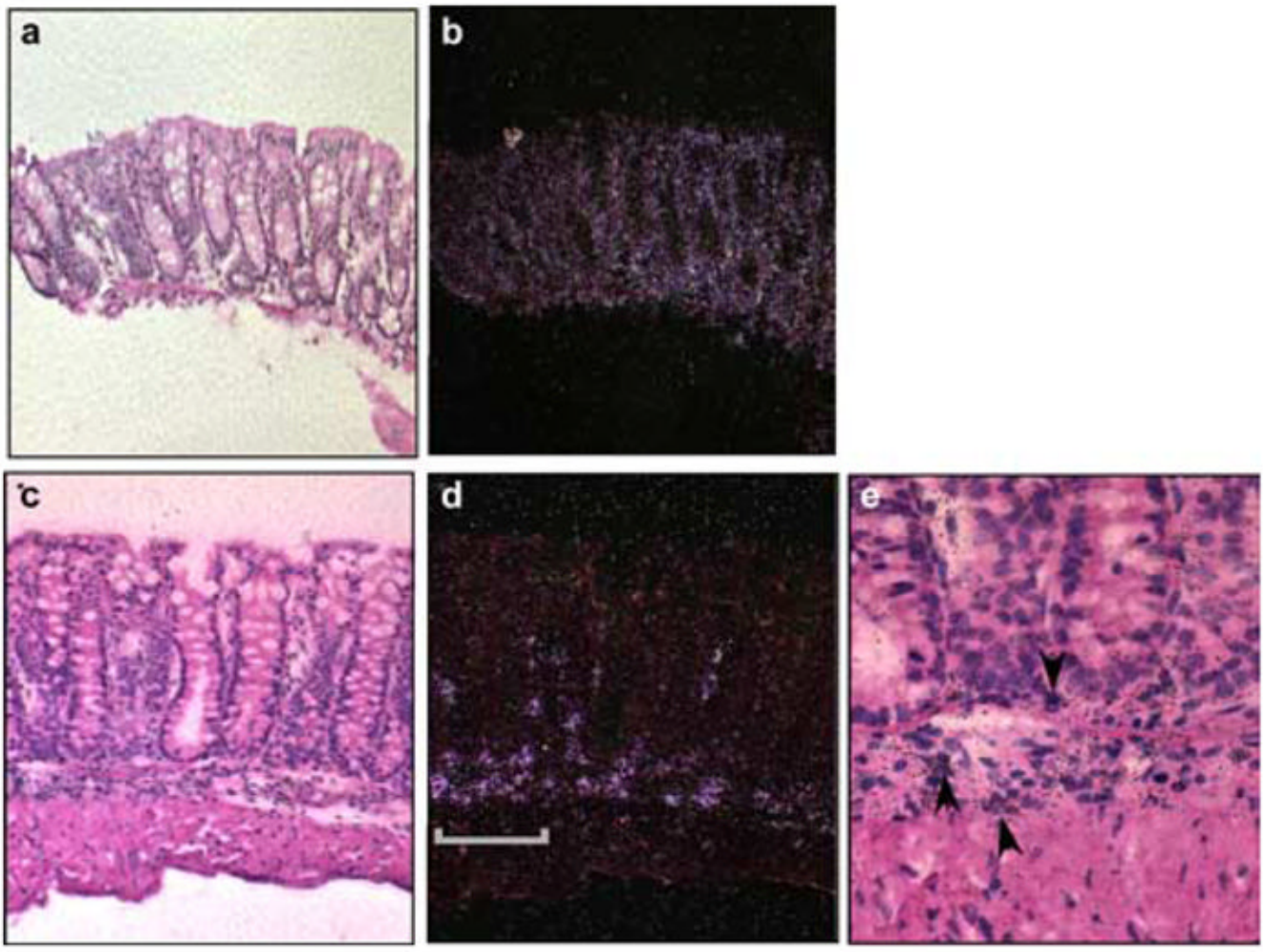

FIGURE 5.

DSS exposure induced mononuclear cell-derived eotaxin-1 mRNA expression. Colonic sections were subjected to in situ hybridization using an eotaxin-1 antisense probe. The hybridization signal of the eotaxin-1 probe is shown in a representative colon from control-treated (*a* and *b*) and DSS-treated (*c* and *e*) mice. Brightfield (*a*, *c*, and *e*) and darkfield (*b* and *d*) images original magnifications of ×100 (*a*–*d*) and ×1000; scale bar = 50 μm (*e*). Arrows indicate eotaxin-1 expression in mononuclear cells (signal grains appear bright in darkfield images and dark in brightfield images).

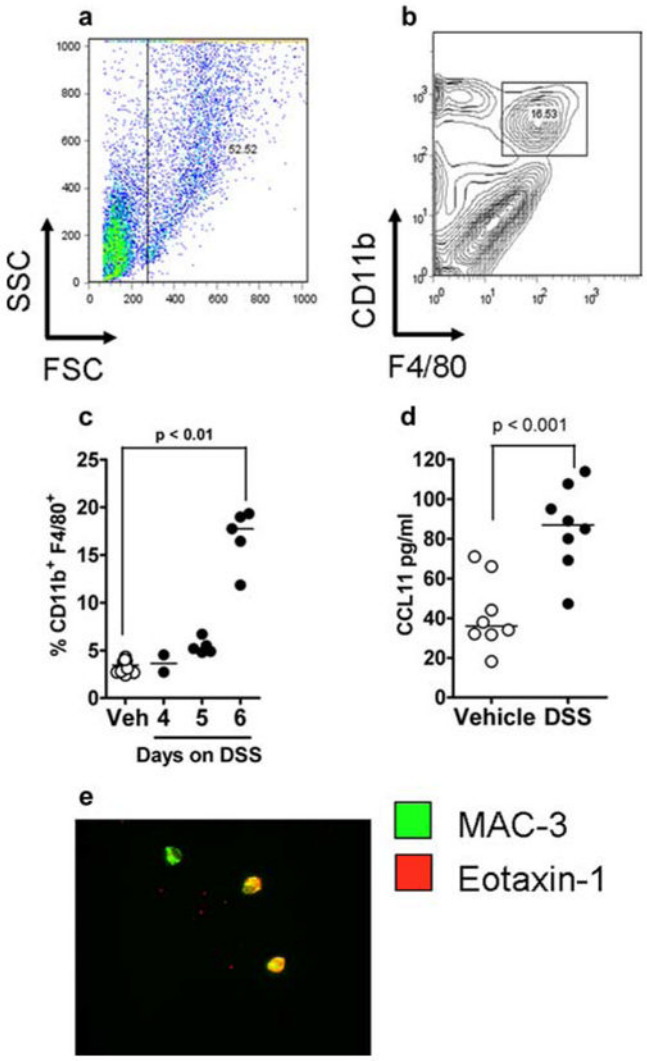

FIGURE 6.

F4/80$^+$ CD11b$^+$ myeloid cells express eotaxin-1 in DSS-induced colitis. *a* and *b*, Flow cytometric identification of intestinal F4/80$^+$ CD11b$^+$ myeloid cells. Representative dot and contour plots of Intestinal F4/80$^+$ CD11b$^+$ myeloid cells identified by FSC^{high}SSC^{high}, F4/80$^+$CD11b$^+$ cells (where FSC is forward scatter and SSC is side scatter). *c*, Levels of intestinal F4/80$^+$CD11b$^+$ myeloid cells in the colon of control (Veh) and 2.5% DSS-treated WT mice. *d*, Eotaxin-1 levels in purified intestinal macrophage homogenates from control (Vehicle) and DSS-treated WT mice. *e*, Immunofluorescence labeling for eotaxin-1 and Mac-3 in adherent purified intestinal macrophages from DSS-treated WT mice. Overlay image of anti-eotaxin-1-Alexa Fluor 594, (green) and anti-Mac-3-Alexa Fluor 488 (red). Original magnification, ×200. *a* and *b*, Representative dot and contour plot from triplicate experiments. *c* and *d*, Individual symbol represents one mouse and the dash represents median value.

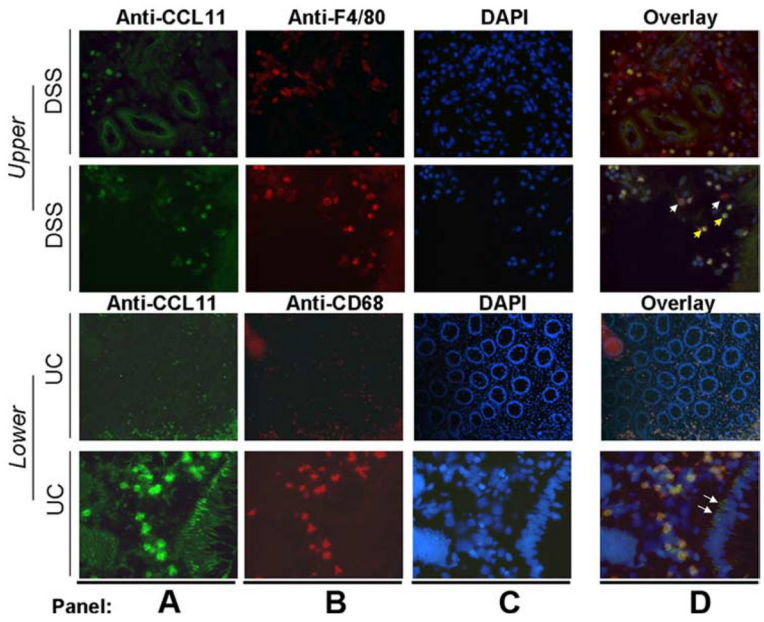

FIGURE 7.

Cellular expression of eotaxin-1 in DSS-induced colitis and UC. *Upper panels*, Immunofluorescence labeling for eotaxin-1 and F4/80 in the colon of DSS-treated WT mice. *A*, Anti-eotaxin-1-Alexa Fluor 594, (green). *B*, Anti-F4/80-Alexa Fluor 488 (red). *C*, Nuclei were stained with DAPI (blue). *D*, Overlay of all *A–C*. Original magnification, ×200. White arrows depict $F4/80^+$ and eotaxin-1^- cells; yellow arrows depict $F4/80^+$ and eotaxin-1^+ cells. *Lower panels*, Immunofluorescence labeling for CD68 and eotaxin-1 in colonic biopsy samples from UC patients. Anti-eotaxin-1-Alexa Fluor 488 is green; anti-CD68-TRITC (red) nuclei were stained with DAPI (blue). Results shown are representative of three cases. Original magnification for top panels was ×50 and that for bottom panels was ×50 and ×200.

Table I

Patient demographics.

	Controls	UC
No. of patients	11	8
Average age (range)	13.5 (6.6 –18.3)	12.3 (6.6 –18.3)
Sex	50% Male	50% Male
UC disease severity		
PUCAI mean (range)	n.a.	40 (10 –75)
Montreal classification	n.a.	9E3, 1E2 and 1E1

[a]PUCAI, pediatric ulcerative colitis clinical activity index; n.a., not applicable; E1, ulcerative proctitis; E2, left-sided UC; E3, extensive UC (extends proximal to splenic flexure).